AIP | Journal of Applied Physics

Adsorbing H2S onto a single graphene sheet: A possible gas sensor

A. H. Reshak and S. Auluck

Citation: Journal of Applied Physics **116**, 103702 (2014); doi: 10.1063/1.4894840
View online: http://dx.doi.org/10.1063/1.4894840
View Table of Contents: http://scitation.aip.org/content/aip/journal/jap/116/10?ver=pdfcov
Published by the AIP Publishing

Adsorbing H_2S onto a single graphene sheet: A possible gas sensor

A. H. Reshak[1,2,a)] and S. Auluck[3]
[1]*New Technologies-Research Centre, University of West Bohemia, Univerzitni 8, 306 14 Pilsen, Czech Republic*
[2]*Center of Excellence Geopolymer and Green Technology, School of Material Engineering, University Malaysia Perlis, 01007 Kangar, Perlis, Malaysia*
[3]*Council of Scientific and Industrial Research-National Physical Laboratory, Dr. K S Krishnan Marg, New Delhi 110012, India*

(Received 15 July 2014; accepted 26 August 2014; published online 8 September 2014)

The electronic structure of pristine graphene sheet and the resulting structure of adsorbing a single molecule of H_2S on pristine graphene in three different sites (bridge, top, and hollow) are studied using the full potential linearized augmented plane wave method. Our calculations show that the adsorption of H_2S molecule on the bridge site opens up a small direct energy gap of about 0.1 eV at symmetry point M, while adsorption of H_2S on top site opens a gap of 0.3 eV around the symmetry point K. We find that adsorbed H_2S onto the hollow site of pristine graphene sheet causes to push the conduction band minimum and the valence band maximum towards Fermi level resulting in a metallic behavior. Comparing the angular momentum decomposition of the atoms projected electronic density of states of pristine graphene sheet with that of H_2S–graphene for three different cases, we find a significant influence of the location of the H_2S molecule on the electronic properties especially the strong hybridization between H_2S molecule and graphene sheet. © *2014 AIP Publishing LLC*. [http://dx.doi.org/10.1063/1.4894840]

I. INTRODUCTION

A honeycomb two dimensional lattice of monolayer carbon atoms, a new material called graphene, was discovered recently.[1,2] Graphene consists of a single atomic layer of sp^2 hybridized carbon atoms that result in a hexagonal lattice. Around each carbon atom, three strong σ bonds are established with the other three surrounding carbon atoms.[3] Research on graphene has opened a new era in nanotechnology. The outstanding mechanical,[4] electrical,[5] and physical properties[6] of graphene warrants its use in a variety of areas such as hydrogen technology,[7] electronics,[5] sensing,[8] and drug delivery,[9,10] among many others. The zero band gap of the graphene at point K renders the construction of graphene based field effect transistors very difficult. Therefore, several groups have proposed different methods to open a band gap in graphene.[11–23] Denis *et al.*[13] found that when graphene is doped with sulfur a band gap is opened depending on the sulfur content. It is found that graphene, which is more accessible to doping and chemical modification at the same time, is more susceptible to structural defects and impurities. Graphene is considered the most promising adsorbent for the adsorption of gases.[24–26] Hegde *et al.*[27] have used the first-principles density functional theory (DFT) to determine the chemical activity of carbon site of pristine graphene, Stone-Wales defect site, and BN-sites of BN-doped graphene towards adsorption of toxic gas H_2S. Recently, DFT calculations were used to investigate the use of transition metal doped carbon nanotubes for chemical gas sensing in pure and modified carbon structures.[28] Castellanos *et al.*[29] and Zhang *et al.*[30] reported DFT studies of adsorption of H_2S on top, bridge, and center sites of graphene. They found that the separation distance between H_2S and graphene sheet is larger than 3.5 Å and H_2S molecules are only physisorbed on graphene. They concluded that H_2S cannot chemically modify the graphene structure and should therefore have little effects on graphene's density of states (DOS). This work motivated us to do more advanced work by changing the separation distance between S atom and the graphene sheet to produce efficient graphene based gas sensor.

In the recent years, research has demonstrated that using carbon nanotubes and semiconductors nanowires results in a novel generation of gas sensors.[31–33] The high acclaim received by the latter materials is due to their exceptional sensitivity allowing the detection of toxic gases in concentrations as small as one part per billion.[34] Schedin *et al.*[33] reported the detection of individual gas molecules adsorbed on graphene. It is based on changes in the electrical conductivity due to gas molecules adsorbed on graphene that act as donors or acceptors.[31,32,34,35] Since graphene is a 2D sheet, it is exposed to surface adsorbates. Also, because it is highly conductive it possesses a low Johnson noise even in the limit of no charge carriers.[36–39] Since H_2S is very malodorous and toxic, it is very important for many chemical applications.[40–42] It is reported that it has damaging effects on many industrial catalysts and is known to be the major source of acid rain when oxidized in the atmosphere.[43] Several industrial processes generate a huge amount of H_2S, including natural gas processing, petroleum refining, coal gasification, biogas fermentation, and the activity of petrochemical plants, Kraft mills, and coke ovens.[43] During the process of the biogas fermentation, a huge amount of H_2S is produced[44–46] because the biogas must be purified from H_2S. Inhaled H_2S is very harmful and can cause death depending on the concentration and the exposure duration.

[a)]Author to whom correspondence should be addressed. Electronic mail: maalidph@yahoo.co.uk. Tel.: +420 777 729 583.

From the above, it is clear that the adsorption of H_2S on graphene is a very important problem. In particular, it is worth exploring which atomic sites favor a good adsorption and the separation distance between H_2S and graphene sheet. Thus, in this work we are interested in investigating the influence of adsorption of a single H_2S molecule onto three different adsorption sites (bridge site in the middle of C-C bond, top site on the top of carbon atom, and hollow site at the center of carbon hexagon), on the electronic structure of pristine graphene sheet. Also, we investigate whether pristine graphene is a good adsorbent material for H_2S molecule or not, in order to use it as a novel generation of small gas molecules sensors. The search for novel adsorbents of small gas molecules is a consequence to the humanity needs for clean environment. As the good sensor properties of graphene nanosheets are unknown till now, it would be worthwhile as a first step to investigate the adsorption of H_2S on different sites of graphene, and to see if graphene nanosheets can be used as efficient sensing materials.

II. STRUCTURAL PROPERTIES AND COMPUTATIONAL DETAILS

To study the electronic structure of pristine graphene and the resulting structure of adsorbing a H_2S molecule on pristine graphene at different sites, the all-electron full potential linearized augmented plane wave (FP-LAPW) method was used to solve the Kohn Sham DFT equations within the framework of the WIEN2k code,[47] with the exchange and correlation energy included through a general gradient approximation in Perdew-Burke-Ernzerhof (GGA-PBE) format.[48] The structure is fully relaxed until the forces on the atoms reach values less than 1 mRy/a.u. Once the forces are minimized in this construction one can then find the self-consistent density at these positions

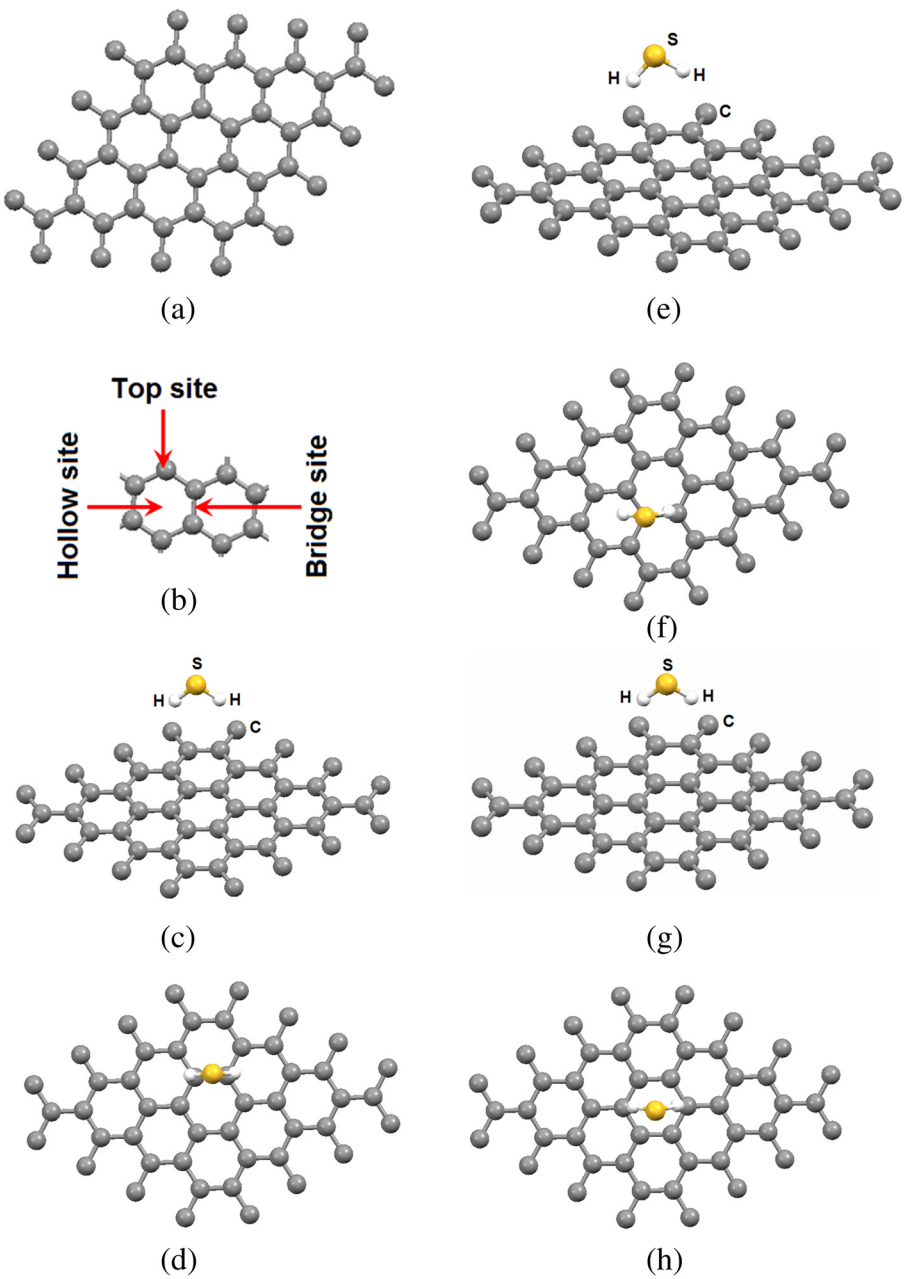

FIG. 1. Schematic view of (a) pristine graphene; (b) three different adsorption sites of H_2S on graphene; (c) H_2S adsorbed onto graphene on the bridge site; (d) H_2S adsorbed onto graphene on the top site; (e) H_2S adsorbed onto graphene on the hollow site.

by turning off the relaxations and driving the system to self-consistency. From the obtained relaxed geometry, the electronic structure and the chemical bonding can be determined and various spectroscopic features can be simulated and compared with experimental data.

For the case of pristine graphene, we have studied three possible adsorption sites namely; bridge site in which H_2S adsorbed in the middle of C-C bond with S-C separation distance 3.38 Å (Fig. 1(c)), top site on the top of carbon atom with S-C separation distance 3.36 Å (Fig. 1(d)), and the hollow site at the center of the carbon hexagon with S-C separation distance 3.34 Å (Fig. 1(e)).

In order to achieve the self-consistency, the values of non-overlapping spheres of muffin-tin radius (R_{MT}) as 1.33 a.u. for C at pristine graphene (4×4) sheet, 1.27, 1.55, and 0.83 a.u. for C, S, and H atoms, respectively, at top-, bridge-, and hollow-sites of adsorbed H_2S onto graphene. These values were chosen in such a way that the spheres did not overlap. In order to achieve sufficient energy convergence, the wavefunctions in the interstitial regions were expanded in plane waves with a cutoff $K_{max} = 7.0/R_{MT}$, where R_{MT} denotes the smallest atomic sphere radius and K_{max} gives the magnitude of the largest K vector in the plane wave basis expansion. The maximum value of $\boldsymbol{l}$ was taken as $\boldsymbol{l}_{max} = 10$, while the charge density is Fourier expanded up to $G_{max} = 20$ (a.u.)$^{-1}$. Self-consistency is obtained using 300 **k**-points in the irreducible Brillouin zone (IBZ). For calculating the total and the angular momentum decomposition of the atoms projected electronic density of states, a denser mesh of 800 **k**-points was used. The self-consistent calculations are considered to be converged when the total energy of the system is stable within 10^{-5} Ry.

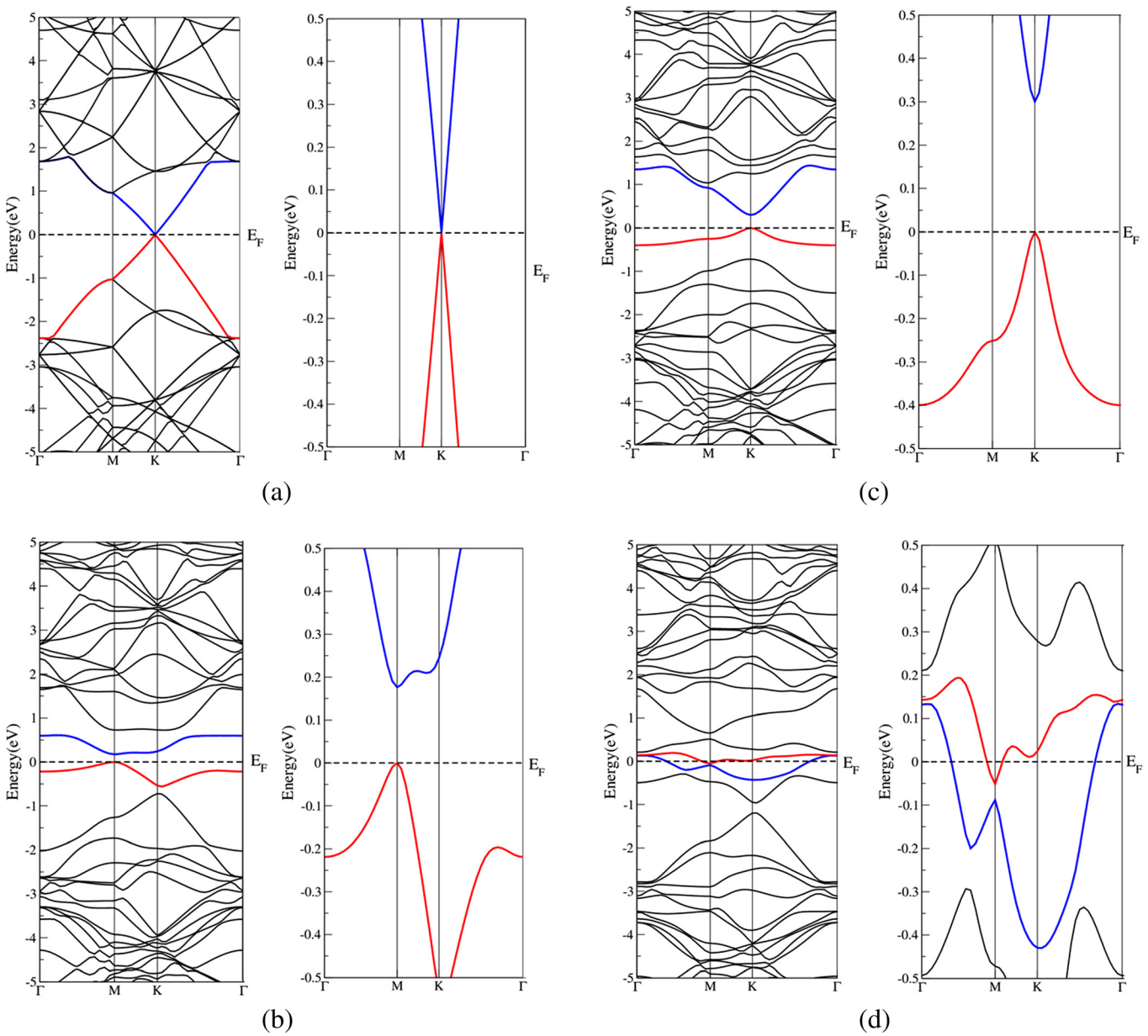

FIG. 2. Calculated electronic band structure.

III. RESULTS AND DISCUSSION

A. Electronic band structure, density of states, and electronic charge density

The geometry of the atomic configurations of pristine graphene (Fig. 1(a)) and three possible adsorption sites of H_2S single molecule onto pristine graphene: bridge site (Figs. 1(b) and 1(c)), top site (Figs. 1(b) and 1(d)), and the hollow site (Figs. 1(b) and 1(e)) were used in this study. We should emphasize that the most stable adsorption configuration is the one with the lowest total energy and the highest adsorption energy among other adsorption sites.[49] Thus, the top site (total energy $E_{TOT} = -3238.87878541$ Ryd) is the most stable configuration in comparison to hollow ($E_{TOT} = -3238.1058284$ Ryd) and bridge ($E_{TOT} = -3238.79501144$ Ryd).

In Figs. 2(a)–2(d), we have plotted the electronic band structure dispersion of the pristine graphene sheet and the three structures (top, bridge, and hollow) in **k**-space along the high symmetry directions in the irreducible Brillouin zone. Following these figures, one can notice that adsorbed H_2S onto pristine graphene results in change of the electronic band structure. For example, adsorption of H_2S onto bridge site causes a dramatic change of the band dispersions (Fig. 2(b)) with respect to pristine graphene (Fig. 2(a)) and opens a direct small energy gap of about 0.1 eV around Fermi energy (E_F) at M point of BZ. This is attributed to the fact that adsorbed H_2S on bridge site causes strong hybridization between C-p and H-s, S-s/p states at the valence band maximum (VBM) and hence strong covalent bonds, while at the conduction band minimum (CBM) the hybridization is weaker and the bonds too. Also, the Coulomb interaction between H_2S and the two C atoms is weak; the states around E_F repel each others, causing to push the CBM towards higher energy with respect to E_F opening a direct gap. While adsorbing H_2S on the top site causes to push CBM further towards higher energies resulting in a direct energy band gap of about 0.3 eV around K point of BZ (Fig. 2(c)). Adsorbing H_2S on top site causes very strong hybridization between C-p and H-s, S-s/p states at the VBM resulting in very strong covalent bonds, while at the CBM the hybridization is much weaker which leads to weak bonds and very weak Coulomb interaction between H_2S and the one C atom resulting in strong repulsion between the states around E_F, thus causing to push the CBM further towards higher energy with respect to E_F opening a slightly bigger direct gap. The upper valence band (Figs. 2(a)–2(d)) shows a very flat k-dispersion.

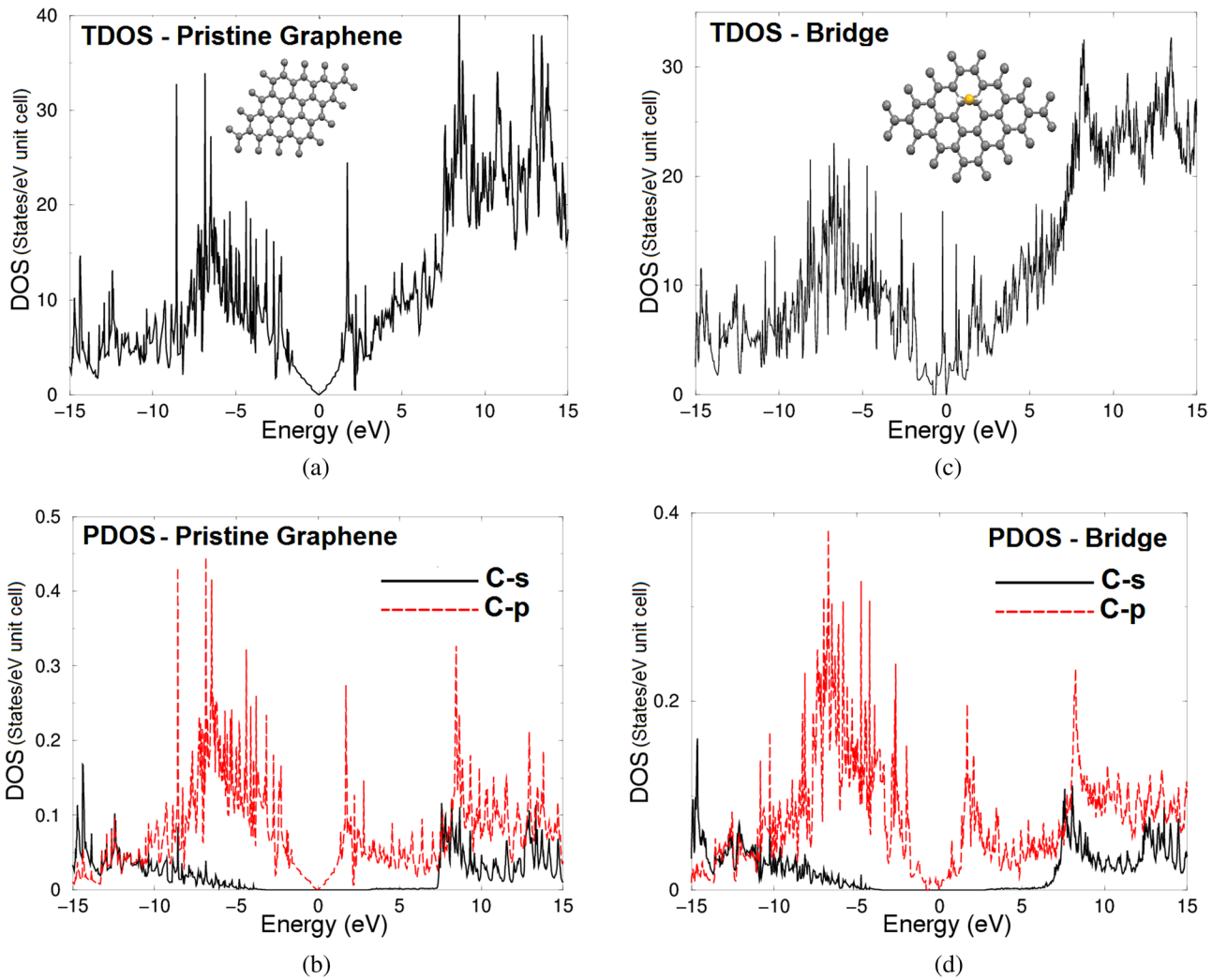

FIG. 3. Calculated total and partial density of states.

This reflects the low mobility of the holes. Our observation of opening a gap around E_F when we adsorb H_2S on the bridge and top site of pristine graphene is consistent with the previous observation of Denis *et al.*[13] They used DFT based SIESTA program within GGA-PBE and found that when graphene is doped with sulfur a band gap is opened depending on the sulfur content.[13]

When H_2S is adsorbed on the hollow site, we notice that both of the CBM and VBM move towards each other and overlap around E_F. This strong overlapping around E_F is due to the fact that in the hollow site the H_2S single molecule is adsorbed onto six C atoms (see Fig. 1(e)). Thus, the H_2S molecule is strongly bonded to six C atoms by strong covalent bonds with equal bond lengths and angles, as there is a strong hybridizations between C-p state and S-s/p and H-s states. Also, this strong overlapping around E_F could be attributed to the strong Coulomb interactions between the single H_2S molecule and the six C atoms resulting in strongly overlap of C-s/p, S-s/p, and H-s states around E_F.

From the total and partial density of states (TDOS and PDOS) of pristine graphene sheet (Figs. 3(a) and 3(b)), it is clear that there is a strong hybridization between C-s and C-p states at the energy region between −9.5 and −8.5 eV, 8.0 eV, and 12.0 eV. The interaction due to the strong hybridization and the covalent bond is defined by the degree of hybridization. Hence, there is a strong covalent bonding between the atoms which exhibit strong hybridization.

Figs. 3(c)–3(k) show the TDOS and PDOS of bridge, top, and hollow site configuration. We should emphasize that adsorbing H_2S onto pristine graphene sheet at three different sites (bridge, top, and hollow) causes a strong hybridization between S-s/p states of H_2S molecule and C-s/p states of the graphene sheet, and hence strong covalent bonds. The TDOS and PDOS of hollow site-configuration suggested that this configuration is metallic, with S-s/p, H-s, and C-p states overlapping around E_F. The DOS at Fermi energy (E_F) is determined by the overlap between the valence and conduction bands. This overlap is strong enough indicating metallic origin with a certain value of DOS at E_F, $N(E_F)$. The density of states at E_F, $N(E_F) = 94.29$ states/Ry cell. The electronic specific heat coefficient (γ), which is function of density of states, can be calculated using the expression

$$\gamma = \frac{1}{3}\pi^2 N(E_F) k_B^2, \tag{1}$$

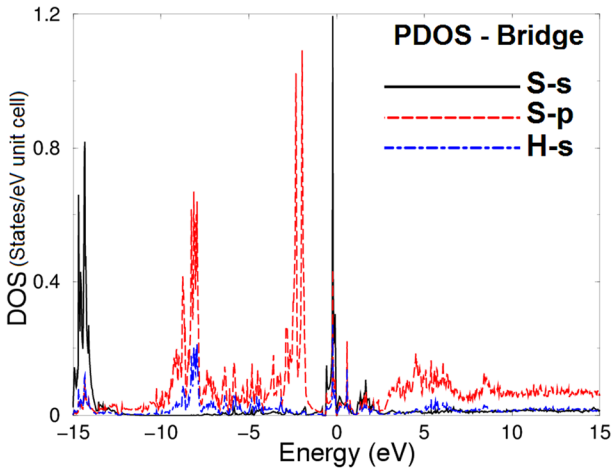

(e)

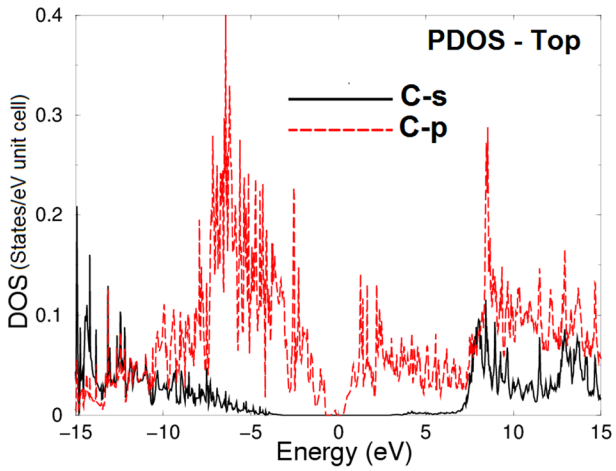

(g)

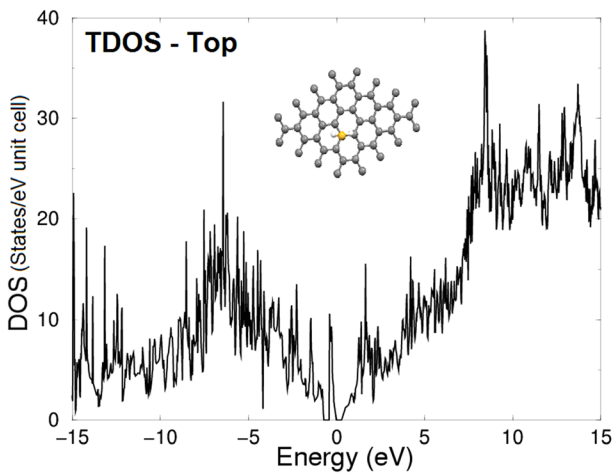

(f)

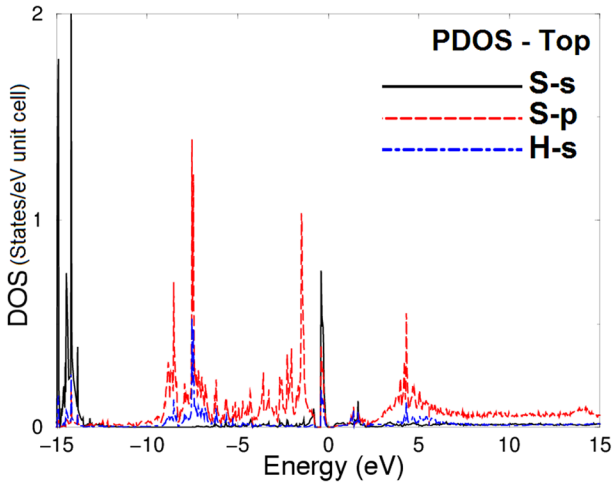

(h)

FIG. 3. (*Continued*).

here $N(E_F)$ is the density of states at Fermi energy, and k_B is the Boltzmann constant. The calculated density of states at Fermi energy $N(E_F)$ enables us to calculate the bare electronic specific heat coefficient. The calculated bare electronic specific heat coefficient is found to be 16.34 mJ/mole K^2 for hollow site configuration. We can list the main features of pristine graphene and the three resulting structures in Table I.

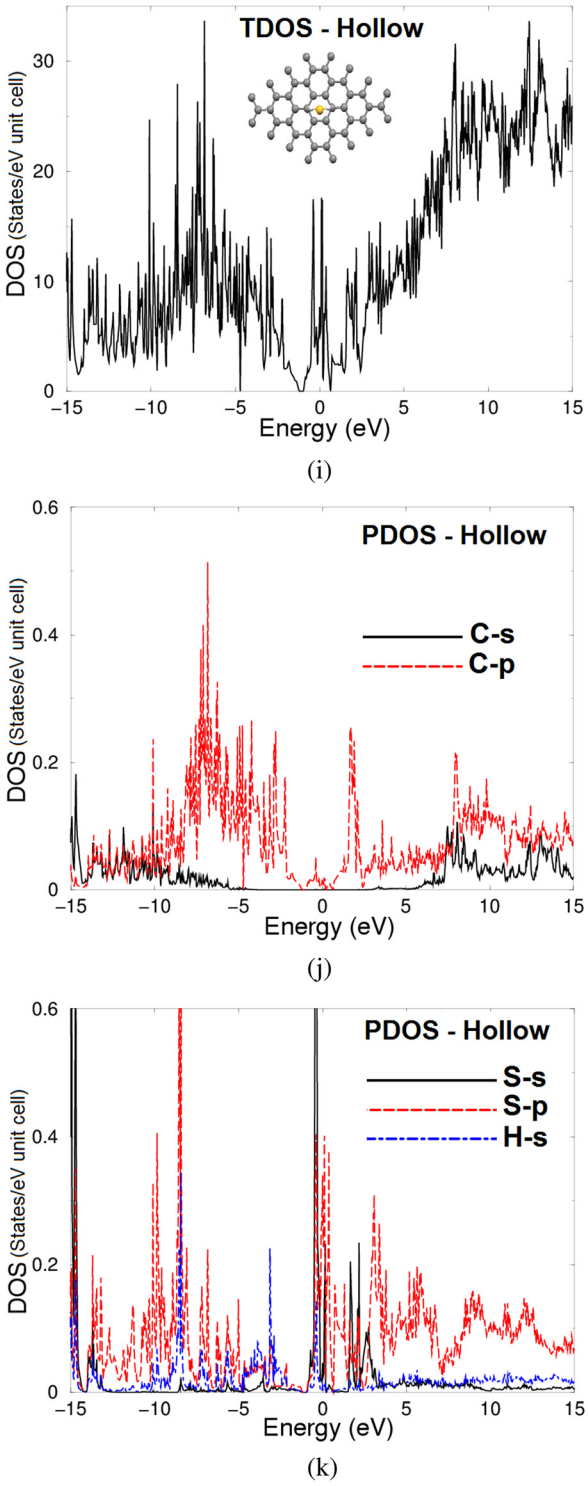

FIG. 3. (*Continued*).

From the PDOS-VB, one can elucidate the origin of chemical bonding following the same method we used in our previous work.[50] One should emphasize that the PDOS-VB located between −10.0 eV and E_F is larger for C-s states (0.3 e/eV) and C-p states (0.02 e/eV) for pristine graphene. C-s states (0.3 e/eV), C-p (0.02 e/eV), S-p states (0.7 e/eV), and H-s states (0.18 e/eV) for the bridge configuration, while for top configuration are C-s states (0.3 e/eV), C-p (0.02 e/eV), S-p states (0.7 e/eV), and H-s states (0.3 e/eV). Finally, for hollow configuration, these numbers are C-s states (0.28 e/eV), C-p (0.05 e/eV), S-p states (0.5 e/eV), and H-s states (0.2 e/eV). Therefore, some electrons from C, H, and S atoms are transferred into valence bands and contribute in covalence interactions. The interaction due to the strong hybridization and the covalent bonds is defined by the degree of hybridization. Hence, there is a strong covalent bonding between the atoms which exhibit strong hybridization. The PDOS help to analyze the nature of the bonds according to a classical chemical concept. This concept is very useful to classify compounds into different categories with respect to different chemical and physical properties. To support this statement, we have taken a more careful look at the bonding situation since the existence of real hybridization between states of atoms should lead to covalent bond's origin between these atoms.

The electronic charge density distribution of pristine graphene sheet and the three configurations (bridge, top, and hollow) has been calculated and shown in Figs. 4(a)–4(d). Fig. 4(a) shows the electron charge density distribution of pristine graphene, one can see that the charge accumulates around C atoms along the bonds and the charge around C atoms is uniformly distributed. This can be seen easily by color charge density scale where blue color (+1.00) corresponds to the maximum charge accumulation site. Also, one can see that there is a strong covalent bonding between the C atoms. The length of the bond is 1.420 Å and the angle between the C atoms is 120°. We should emphasize that in the centre of the honeycomb the charge is zero as can be seen by red color (+0.00), which corresponds to the minimum charge accumulation site.

Figs. 4(b)–4(d) show the electron charge density distribution of bridge, top, and hollow configurations. According to the electronegativity values of C (2.55), S (2.58), and H (2.1), it is clear that there is a strong covalent bonding between C-C atoms and maximum charge accumulates around C atoms along the bonds indicated by blue color (+1.00), the charge around C atoms is uniformly distributed. Also, there is strong charge accumulated around H atoms, blue color (+1.00). There is partial ionic and strong covalent bond between H and S. The density of the charge accumulation around S atoms is less than around C and H atoms according to color charge density scale color (green color corresponds to charge +0.400).

B. Electron effective mass

Electron effective mass for pristine graphene at K point of BZ, bridge at M point of BZ, and top at K point of BZ, respectively, is obtained from the curvature of the

TABLE I. The main features of pristine graphene in comparison to the bridge, top, and hollow sites of H_2S molecule.

Structure	Gap (eV)	CBM	VBM	$N(E_F)$ (states/Ry cell)	γ (mJ/mole K^2)
Pristine graphene	0.0 eV	K	K	0.0	0.0
H_2S on bridge site	0.1	M	M	0.0	0.0
H_2S on top site	0.3 eV	K	K	0.0	0.0
H_2S on hollow site	Metallic	Overlapping around E_F	Overlapping around E_F	94.29	16.34

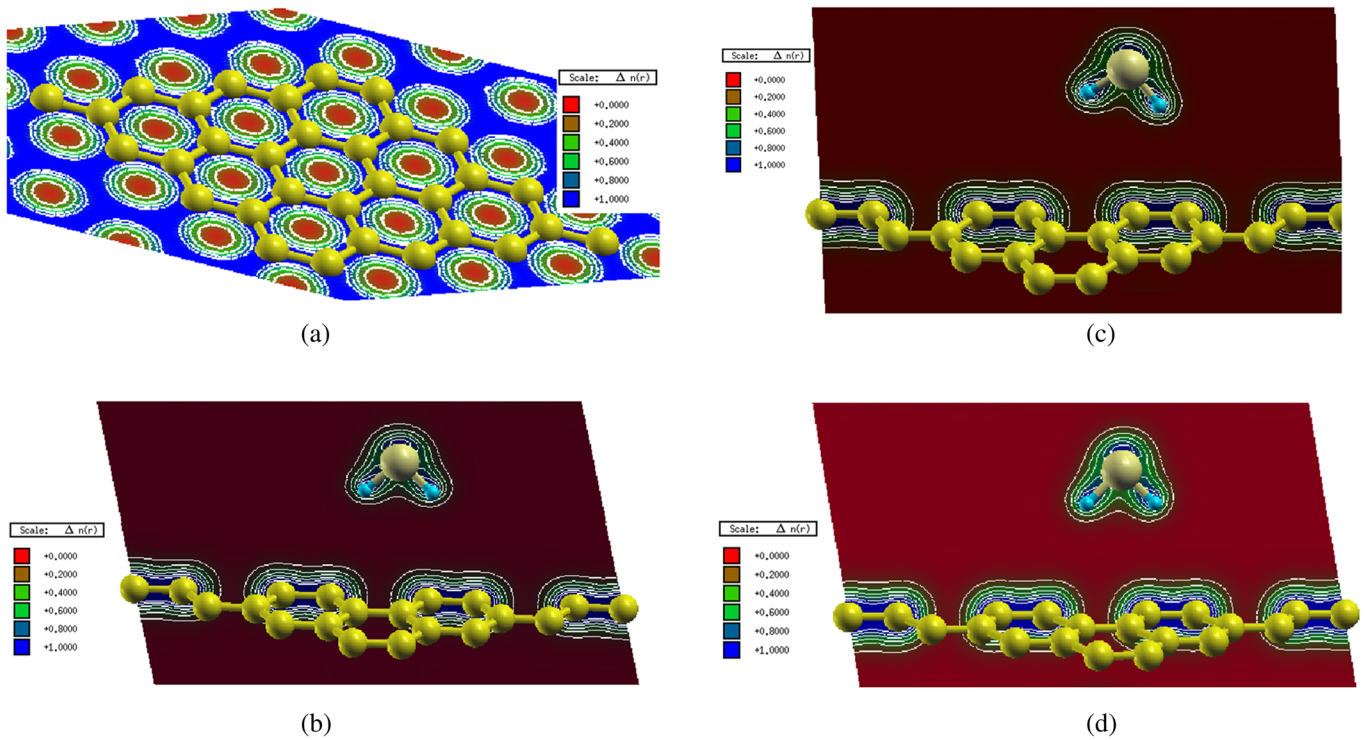

FIG. 4. Calculated electron charge density.

conduction band minimum. To illustrate how the pristine graphene, bridge, and top transition alters the electronic band structure of the host materials, we have enlarged the band structures of pristine graphene, bridge, and top as illustrated in Fig. 2. The electron effective mass has been determined from fitting the electronic band structure to a parabolic function for the six directions in the first Brillouin zone using GGA approaches. The diagonal elements of the effective mass tensor, m_e, for the electrons in the conduction band are calculated around K point in k space using the expression

$$\frac{1}{m_e^*} = \frac{1\partial^2 E(k)}{\hbar^2 \partial k^2}. \quad (2)$$

The values of calculated electron effective mass ratio for pristine graphene at K point of BZ, bridge at M point of BZ, and top at K point of BZ are 0.0025, 0.0047, and 0.0051, respectively. The electron mobility characterizes how quickly an electron can move through a metal or semiconductor. The electron effective mass values are maximum in the top configuration than the other two configurations. Also, we have calculated the effective mass ratio of the heavy holes (light holes) for pristine graphene at K point of BZ, bridge at M point of BZ, and top and K point of BZ, these values are 0.0019 (0.0031), 0.0050 (0.0019), and 0.0079 (0.0068).

IV. CONCLUSIONS

DFT calculations based on all-electron FP-LAPW method were performed to investigate the electronic structure of pristine graphene and three different adsorption sites of H_2S onto graphene. In order to understand the adsorption properties of H_2S molecule adsorbed onto graphene, three possible adsorption configurations (top, bridge, and hollow) were considered with S-C separation distance varying between 3.38 and 3.34 Å. Calculations show that the adsorption of H_2S on bridge and top sites opens very small direct energy gap, whereas adsorbing H_2S on hollow site cause to close the gap resulting in metallic behavior. The angular momentum decomposition of the atoms projected electronic density of states of pristine graphene and of H_2S-pristine graphene for three different sites (top, bridge, and hollow) confirms that there is a strong hybridization between H_2S molecule and graphene sheet. We should emphasize that the

strong hybridization between H_2S molecule and pristine graphene sheet results in dramatic changes in the electronic properties. Therefore, the interaction of H_2S with graphene shows very strong physical adsorption and hence different physical properties. Thus, pristine graphene is very good adsorbent materials for H_2S molecule.

In summary, the pristine graphene sheet is a zero gap semiconductor, while when a single H_2S molecule adsorb onto pristine graphene, we find that the bridge and top become direct gap semiconductors (0.1 and 0.3 eV), whereas the hollow case is metallic, where S-s/p, H-s, and C-p states control the overlapping around E_F. The DOS at E_F is determined by the overlap between the valence and conduction bands. This overlap is strong enough indicating metallic origin with certain value of DOS at E_F, $N(E_F) = 94.29$ states/Ry cell, for hollow site configuration. The electronic specific heat coefficient (γ), which is function of DOS, can be obtained from $N(E_F)$. Thus, the calculated bare electronic specific heat coefficient is found to be 16.34 mJ/mole K^2 for hollow.

Adsorbing a single molecule of H_2S onto pristine graphene at the hollow sites causes change to pristine graphene from zero-gap semiconductor to metallic with two bands cuts Fermi level. Therefore, we have calculated the Fermi surface of the new configuration. Fermi surface topology is due to changes in inter-atomic distances, bonding angles as well as to the degree of band filling.

ACKNOWLEDGMENTS

The result was developed within the CENTEM project, Reg. No. CZ.1.05/2.1.00/03.0088, co-funded by the ERDF as part of the Ministry of Education, Youth and Sports OP RDI program. Computational resources were provided by MetaCentrum (LM2010005) and CERIT-SC (CZ.1.05/3.2.00/08.0144) infrastructures. S.A. thanks Council of Scientific and Industrial Research (CSIR)-National Physical Laboratory for financial support.

[1]K. Nakada, M. Fujita, G. Dresselhaus, and M. S. Dresselhaus, Phys. Rev. B **54**, 17954 (1996).
[2]S. Okada, Phys. Rev. B **77**, 041408 (2008).
[3]R. Lv and M. Terrones, Mater. Lett. **78**, 209–218 (2012).
[4]C. Gomez-Navarro, M. Burghard, and K. Kern, Nano Lett. **8**, 2045 (2008).
[5]Y.-H. Lin, K. A. Jenkins, A. Valdes-Garcia, J. P. Small, D. B. Farmer, and P. Avouris, Nano Lett. **9**, 422 (2009).
[6]C. L. Kane and E. J. Mele, Phys. Rev. Lett. **95**, 226801 (2005).
[7]A. Ferre-Vilaplana, J. Chem. Phys. **122**, 104709 (2005).
[8]I. Zanella, S. B. Fagan, R. Mota, and A. Fazzio, J. Phys. Chem. C **112**, 9163 (2008).
[9]Z. Liu, J. T. Robinson, X. Sun, and H. Dai, J. Am. Chem. Soc. **130**, 10876 (2008).
[10]A. de Leon and A. F. Jalbout, Chem. Phys. Lett. **457**, 179 (2008).
[11]R. M. Ribeiro, N. M. R. Peres, J. Coutinho, and P. R. Briddon, Phys. Rev. B **78**, 075442 (2008).
[12]E. Bekyarova, M. E. Itkis, P. Ramesh, C. Berger, M. Sprinkle, W. A. De Heer, and R. C. Haddon, J. Am. Chem. Soc. **131**, 1336 (2009).
[13]P. A. Denis, R. Faccio, and A. W. Mombru, ChemPhysChem **10**, 715 (2009).
[14]D. C. Elias, R. R. Nair, T. M. G. Mohiuddin, S. V. Morozov, P. Blake, M. P. Halshall, A. C. Ferrari, D. W. Boukhvalov, M. I. Katsnelson, A. K. Geim, and K. S. Novoselov, Science **323**, 610 (2009).
[15]J. O. Sofo, A. S. Chaudhari, and G. D. Barber, Phys. Rev. B **75**, 153401 (2007).
[16]S. Casolo, O. L. Lovnik, R. Martinazzo, and G. F. Tantardini, J. Chem. Phys. **130**, 054704 (2009).
[17]D. W. Boukhvalov, M. I. Katsnelson, and A. I. Lichtenstein, Phys. Rev. B **77**, 035427 (2008).
[18]X. Sha and B. Jackson, Surf. Sci. **496**, 318 (2002).
[19]L. Hornekaer, E. Rauls, W. Xu, Z. Sljivancanin, R. Otero, I. Steensgaard, E. Laegsgaard, B. Hammer, and F. Besenbacher, Phys. Rev. Lett. **96**, 156104 (2006).
[20]Y. Ferro, F. Marinelli, and A. Allouche, Chem. Phys. Lett. **368**, 609 (2003).
[21]T. Roman, W. A. Dino, H. Nakanishi, H. Kasai, T. Sugimoto, and K. Tange, Carbon **45**, 218 (2007).
[22]L. Chen, A. C. Copper, C. P. Pez, and H. Cheng, J. Phys. Chem. C **111**, 18995 (2007).
[23]P. O. Lehtinen, A. S. Foster, Y. Ma, A. V. Krasheninnikov, and R. M. Nieminen, Phys. Rev. Lett. **93**, 187202 (2004).
[24]M. Suzuki, "Activated carbonfiber: Fundamentals and applications," Carbon **32**, 577–586 (1994).
[25]J. Zhao, A. Buldum, J. Han, and J. P. Lu, "Gas molecule adsorption in carbon nanotubes and nanotube bundles," Nanotechnology **13**, 195–200 (2002).
[26]P. Bondavalli, P. Legagneux, and D. Pribat, "Carbon nanotubes based transistors as gas sensors: State of the art and critical review," Sens. Actuators, B **140**, 304–318 (2009).
[27]V. I. Hegde, S. N. Shirodkar, N. Tit, U. V. Waghmare, and Z. H. Yamani, Surf. Sci. **621**, 168–174 (2014).
[28]J. M. Garcia-Lastra, D. J. Mowbray, K. S. Thygesen, A. Rubio, and K. W. Jacobsen, "Computational design of chemical nanosensors: Metal doped carbon nanotubes," Phys. Rev. B **81**, 245429 (2010).
[29]J. E. Castellanos Aguila, H. Hernandez Cocoletzi, and G. Hernandez Cocoletzi, AIP Adv. **3**, 032118 (2013).
[30]Y.-H. Zhang, L.-F. Han, Y.-H. Xiao, D.-Z. Ja, Z.-H. Guo, and F. Li, Comput. Mater. Sci. **69**, 222–228 (2013).
[31]J. Kong *et al.*, "Nanotube molecular wires as chemical sensors," Science **287**, 622–625 (2000).
[32]P. G. Collins, K. Bradley, M. Ishigami, and A. Zettl, "Extreme oxygen sensitivity of electronic properties of carbon nanotubes," Science **287**, 1801–1804 (2000).
[33]F. Schedin, A. K. Geim, S. V. Morozov, E. W. Hill, P. Blake, M. I. Katsnelson, and K. S. Novoselov, Nature Mater. **6**, 652–655 (2007).
[34]P. T. Moseley, "Solid state gas sensors," Meas. Sci. Technol. **8**, 223–237 (1997).
[35]S. Capone, A. Forleo, L. Francioso, R. Rella, P. Siciliano, J. Spadavecchia, D. S. Presicce, and A. M. Taurino, "Solid state gas sensors: State of the art and future activities," J. Optoelectron. Adv. Mater. **5**, 1335–1348 (2003).
[36]A. K. Geim and K. S. Novoselov, "The rise of grapheme," Nature Mater. **6**, 183–191 (2007).
[37]K. S. Novoselov *et al.*, "Two dimensional atomic crystals," Proc. Natl. Acad. Sci. U.S.A. **102**, 10451–10453 (2005).
[38]K. S. Novoselov *et al.*, "Two dimensional gas of massless Dirac fermions in graphene," Nature **438**, 197–200 (2005).
[39]Y. Zhang, J. W. Tan, H. L. Stormer, and P. Kim, "Experimental observation of the quantum Hall effect and Berry's phase in graphene," Nature **438**, 201–204 (2005).
[40]P. Forzatti and L. Lietti, "Catalyst deactivation," Catal. Today **52**, 165–181 (1999).
[41]Y. Xiao, Sh. Wang, D. Wu, and Q. Yuan, "Catalytic oxidation of hydrogen sulfide over unmodified and impregnated activated carbon," Sep. Purif. Technol. **59**, 326–332 (2008).
[42]Y. Elsayed, M. Seredych, A. Dallas, and T. J. Bandosz, "Desulfurization of air at high and low H_2S concentrations," Chem. Eng. J. **155**, 594–602 (2009).
[43]M. Darvish Ganji, N. Sharifi, M. Ardjmand, and M. Ghorbanzadeh Ahangari, Appl. Surf. Sci. **261**, 697–704 (2012).
[44]P. Cosoli, M. Ferrone, S. Pricl, and M. Fermeglia, "Hydrogen sulphide removal from biogas by zeolite adsorption. Part I. GCMC molecular simulations," Chem. Eng. J. **145**, 86–92 (2008).
[45]S. Mubeen, T. Zhang, N. Chartuprayoon, Y. Rheem, A. Mulchandani, N. V. Myung, and M. A. Deshusses, "Sensitive detection of $_{H2S}$ using gold nanoparticle decorated single-walled carbon nanotubes," Anal. Chem. **82**, 250–257 (2010).

[46]S. Nishimura and M. Yoda, "Removal of hydrogen sulfide from an anaerobic biogas using a bio-scrubber," Water Sci. Technol. **36**, 349–356 (1997).
[47]P. Blaha, K. Schwarz, G. K. H. Madsen, D. Kvasnicka, and J. Luitz, *WIEN2K: An Augmented Plane Wave + Local Orbitals Program for Calculating Crystal Properties* (Techn. Universitat, Wien, Austria, 2001).
[48]J. P. Perdew, S. Burke, and M. Ernzerhof, Phys. Rev. Lett. **77**, 3865–3868 (1996).
[49]M. Zhou, Y.-H. Lu, Y.-Q. Cai, C. Zhang, and Y.-P. Feng, Nanotechnology **22**, 385502 (2011).
[50]A. H. Reshak, D. Stys, S. Auluck, and H. Kamarudin, Mater. Chem. Phys. **130**, 458 (2011).